A pure $S = 3/2$ $[Fe_4S_4]^+$ cluster in the A33Y variant of *Pyrococcus furiosus* ferredoxin

Randall E. Duderstadt, Phillip S. Brereton, Michael W.W. Adams, Michael K. Johnson*

Departments of Chemistry, and Biochemistry and Molecular Biology, and the Center for Metalloenzyme Studies, University of Georgia, Athens, GA 30602, USA

Received 12 April 1999; received in revised form 25 May 1999

Abstract The properties of the $[4Fe\text{-}4S]^{2+/+}$ cluster in wild-type and the A33Y variant of *Pyrococcus furiosus* ferredoxin have been investigated by the combination of EPR, variable-temperature magnetic circular dichroism (VTMCD) and resonance Raman (RR) spectroscopies. The A33Y variant involves the replacement of an alanine whose α-C is less than 4 Å from one of the cluster iron atoms by a tyrosine residue. Although the spectroscopic results give no indication of tyrosyl cluster ligation, the presence of a tyrosine residue in close proximity to the cluster results in a 38-mV decrease in the midpoint potential of the $[4Fe\text{-}4S]^{2+,+}$ couple and has a marked effect on the ground state properties of the reduced cluster. The mixed spin $[4Fe\text{-}4S]^+$ cluster in the wild-type protein, 80% $S = 3/2$ ($E/D = 0.22$, $D = +3.3$ cm^{-1}) and 20% $S = 1/2$ ($g = 2.10, 1.87, 1.80$), is converted into a homogeneous $S = 3/2$ ($E/D = 0.30$, $D = -0.7$ cm^{-1}) form in the A33Y variant. As the first example of a pure $S = 3/2$ $[4Fe\text{-}4S]^+$ cluster in a ferredoxin, this variant affords the opportunity for detailed characterization of the excited electronic properties via VTMCD studies and demonstrates that the protein environment can play a crucial role in determining the ground state properties of $[4Fe\text{-}4S]^+$ clusters.

Key words: Ferredoxin; Iron-sulfur cluster; *Pyrococcus furiosus*; EPR; Magnetic circular dichroism; Resonance Raman

1. Introduction

Prior to the discovery of $S = 3/2$ $[4Fe\text{-}4S]^+$ clusters in the Mo-nitrogenase Fe protein in 1985 [1–3], all $[4Fe\text{-}4S]^+$ clusters were considered to have $S = 1/2$ ground states. Since then, EPR, often in conjunction with VTMCD studies, has been used to identify $S = 3/2$ $[4Fe\text{-}4S]^+$ clusters in wide variety of enzymes and proteins, e.g. *Escherichia coli* fumarase A [4], *E. coli* dihydroxy-acid dehydratase [5], *Bacillus subtilis* phosphoribosylpyrophosphate amidotransferase [6], V-nitrogenase Fe protein [7], *Clostridium pasteurianum* hydrogenase I [8], *Pyrococcus furiosus* ferredoxin:aldehyde oxidoreductase (AOR) [9], *Desulfovibrio africanus* FdIII [10] and *P. furiosus* Fd [11]. For $[4Fe\text{-}4S]^+$ clusters ligated by a Fd-like arrangement of four cysteine residues, i.e. -C-X_2-C-X_2-C- and a remote -C-P-, the ground state is invariably $S = 1/2$. Prior to this work, there were no examples of $[4Fe\text{-}4S]^+$ clusters ligated by a Fd arrangement of coordinating residues that had pure $S = 3/2$ ground states, but clusters having a physical mixture of $S = 1/2$ and 3/2 ground states have been observed in cases where one of these cysteines is replaced by an oxygenic ligand such as aspartate [10,11] or serinate [12]. However, for clusters with alternative primary sequence arrangements of coordinating cysteines, there are several examples of $[4Fe\text{-}4S]^+$ clusters with complete cysteinyl ligation that have mixed spin ($S = 1/2$ and 3/2) ground states [6,7] as well as examples with homogeneous $S = 1/2$ or $S = 3/2$ ground states [9].

Numerous structurally characterized synthetic analogs of the type $[Fe_4S_4(SR)_4]^{3-}$ have been investigated by Holm and co-workers [13,14]. Their findings reveal the presence of an $S = 3/2$ component in most polycrystalline samples, and in all samples once dissolved in dimethylformamide solution. Three different categories of ground state spin behavior were identified: (a) pure $S = 1/2$ or $S = 3/2$ states; (b) physical mixtures of $S = 1/2$ and $S = 3/2$ states; (c) quantum mechanical spin admixture states ($S = 1/2+3/2$) with properties that cannot be rationalized in terms of either (a) or (b). The first biological example of a 'spin-admixed' $[4Fe\text{-}4S]^+$ cluster was recently reported in the inappropriately named 'prismane' protein from *Desulfovibrio vulgaris* [15]. However, no obvious relationships between core distortion, terminal ligand conformation and spin state have emerged from the extensive studies of these analog complexes.

P. furiosus Fd is a small monomeric protein (7.5 kDa) containing a single $[4Fe\text{-}4S]^{2+,+}$ cluster that is remarkable for its extreme thermal stability (stable at 95°C for at least 7 days without significant degradation) and in being the only example of a 4Fe Fd in which one of the cysteinate cluster ligands is replaced by an aspartate [11,16]. In this work we report on the preparation and spectroscopic characterization of the A33Y variant of *P. furiosus* 4Fe Fd. The 3-dimensional (3D) solution structure[1] as deduced by NMR studies of the D14C mutant which contains an all cysteinyl ligated $[4Fe\text{-}4S]^{2+}$ cluster [17], indicates that the Cγ of A33 is 3.8 Å from the cluster. Previous spectroscopic studies of the A33C mutant revealed medium-dependent changes in the properties of the $[3Fe\text{-}4S]^+$ cluster that were attributed to cluster ligation by the additional cysteine [18]. In the case of the A33Y variant, the recombinant Fd contains a $[4Fe\text{-}4S]^{2+,+}$ cluster as purified from *E. coli* and there is no spectroscopic evidence for tyrosyl cluster ligation. However, the placement of a tyrosyl residue in close proximity to the cluster perturbs the redox potential of the $[4Fe\text{-}4S]^{2+,+}$ couple and the ground state properties of the $[4Fe\text{-}4S]^+$ cluster, affording the first example of a homogeneous $S = 3/2$ $[4Fe\text{-}4S]^+$ cluster in a Fd.

*Corresponding author. Department of Chemistry, University of Georgia, Athens, GA 30602, USA. Fax: +1 (706) 542-2353. E-mail: johnson@sunchem.chem.uga.edu

[1] Calzolai, L., Gorst, C.M., Bren, K.L., Zhou, Z.H., Adams, M.W.W., and La Mar, G.N., manuscript in preparation.

PII: S0014-5793(99)00766-8

2. Materials and methods

2.1. Protein samples

Wild-type *P. furiosus* Fd was purified as previously described [16]. The recombinant A33Y mutant form was constructed, expressed in *E. coli* and purified anaerobically in its 4Fe form using the methodology described in detail in previous publications [12,19,20]. Samples were stored as frozen pellets in 100 mM Tris-HCl buffer, pH 7.8, with 2 mM sodium dithionite added, and handled under Argon in a Vacuum Atmospheres glove box (<1 ppm O_2) unless otherwise indicated. Oxidized samples were prepared by brief exposure to air after removal of excess dithionite by ultrafiltration buffer exchange. Protein concentrations were determined using a modified Lowry method after precipitation with trichloroacetic acid (10% w/v) [16]. Reduction potentials were determined by cyclic voltammetry at a glassy carbon electrode as previously described [12], using an electrochemical cell identical to that designed by Hagen [21].

2.2. Spectroscopic methods

VTMCD spectra were recorded on samples containing either 50% (v/v) glycerol or 55% (v/v) polyethylene glycol (PEG) using a Jasco J715 (180–1000 nm) spectropolarimeter mated to an Oxford Instruments SM-3 (1.5–300 K, 0–5 T) or Spectromag 4000 (1.5–300 K, 0–7 T) split-coil superconducting magnet. The MCD intensities are expressed as $\Delta\varepsilon$ ($\varepsilon_{LCP}-\varepsilon_{RCP}$), where ε_{LCP} and ε_{RCP} are the molar extinction coefficients for the absorption of left and right circularly polarized light, respectively, and are corrected for strain-induced depolarization and natural CD [22,23]. Perpendicular mode X-band ($\sim$9.6 GHz) EPR spectra were obtained using a Bruker ESP-300E EPR spectrometer equipped with an Oxford Instruments ESR-9 flow cryostat, and quantified under non-saturating conditions using a 1 mM Cu (EDTA) standard.

Resonance Raman spectra were recorded with an Instruments SA U1000 spectrometer fitted with a cooled RCA 31034 photomultiplier tube, using lines from a Coherent Innova 100 10-W Ar^+ laser. Scattering was collected at 90° from the surface of a frozen 10-μl droplet of protein solution using a custom-designed, gold-plated, anaerobic sample holder [24] attached to the cold finger of an Air Products Displex model CSA-202E closed cycle refrigerator. Band positions were calibrated using the excitation wavelength and verified using a concentrated Na_2SO_4 reference solution, and are accurate to ± 0.5 cm^{-1}. A spectrum of the frozen buffer solution, normalized to the intensity of the ice-band at 231 cm^{-1} which serves as an internal standard, and a liner ramp fluorescent background have been subtracted from all spectra shown.

3. Results

3.1. Redox properties

The midpoint potential for the reduction of the $[4Fe\text{-}4S]^{2+,+}$ couple in A33Y *P. furiosus* Fd was determined to be -406 mV versus NHE (pH 7.0, 23°C) by cyclic voltammetry at a glassy carbon electrode in the presence of the promoter neomycin. This potential is lower by 38 mV than that of the WT Fd under identical conditions ($E_m = -368$ mV), and was almost invariant to pH over the range pH 3–10.

3.2. EPR

The EPR spectra of wild-type (WT) and A33Y *P. furiosus* Fd as purified in the presence of sodium dithionite are compared in Fig. 1. A detailed analysis of the WT Fd EPR has been presented in previous work [11]. Although the spectrum appears to be dominated by a near-axial $S = 1/2$ resonance ($g = 2.10$, 1.87, 1.80), spin quantitations indicate that the $S = 1/2$ component corresponds to only 20–25% of the $[4Fe\text{-}4S]^+$ clusters. The remaining clusters give rise to a broad $S = 3/2$ resonance spanning at least 600 mT, with the low-field features centered at $g = 5.6$ and 5.00 as the most readily detected components. Temperature-dependent studies

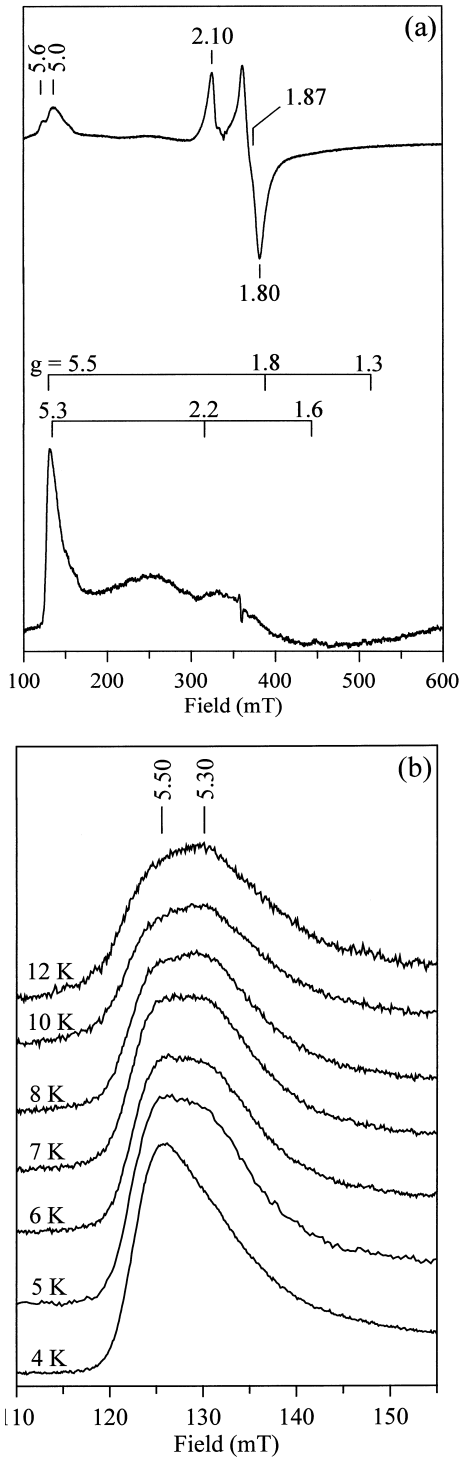

Fig. 1. a: Perpendicular mode X-band EPR spectra of dithionite-reduced WT (top) and A33Y (bottom) *P. furiosus* 4Fe Fd. The samples, 0.75 mM in Fd, were in 50 mM Tris-HCl buffer, pH 7.8, with 2 mM sodium dithionite. Conditions of measurement: temperature, 4.2 K; microwave frequency, 9.61 GHz; modulation amplitude, 0.64 mT; microwave power, 1 mW (WT) and 10 mW (A33Y). b: Temperature dependence of the low-field component in the EPR spectrum of the A33Y variant.

and analysis with a conventional spin Hamiltonian of the form

$$\mathcal{H}_e = g_0\beta \boldsymbol{H}\cdot\boldsymbol{S} + D(\boldsymbol{S}_z^2 - S(S+1)/3) + E(\boldsymbol{S}_x^2 - \boldsymbol{S}_y^2)$$

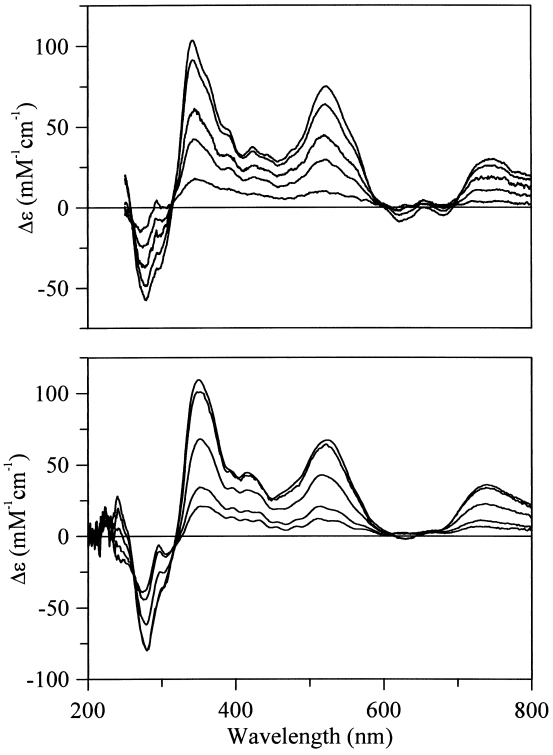

Fig. 2. UV-visible VTMCD spectra of dithionite-reduced WT and A33Y *P. furiosus* 4Fe Fd. Both samples were in 100 mM Tris-HCl buffer, pH 7.8, with 2 mM sodium dithionite and 50% (v/v) glycerol (WT) or 55% (v/v) polyethylene glycol (A33Y). Upper panel: Wild-type, 0.35 mM in Fd; MCD spectra recorded with a magnetic field of 4.5 T at 1.60 K, 4.22 K, 9.1 K, 14.8 K and 50 K. Lower panel: A33Y, 0.34 mM in Fd; MCD spectra recorded with a magnetic field of 6 T at 1.63 K, 4.22 K, 9.7 K, 23.6 K, 42 K. For both samples, the MCD intensity at all wavelengths increases in intensity with decreasing temperature.

where D and E are the axial and rhombic zero-field splitting parameters, indicates $E/D = 0.22$ and $D = +3.3 \pm 0.2$ cm^{-1}. For $g_0 = 1.98$, these parameters predict a zero-field split ground state consisting of a lower doublet with $g = 5.05$, 2.61, 1.72 separated by ~ 7 cm^{-1} from an upper doublet with $g = 5.56$, 1.35, 1.09. Although the addition of 50% (v/v) glycerol or ethylene glycol (as used for VTMCD studies) does not significantly alter the properties of either the $S = 1/2$ or $S = 3/2$ [4Fe-4S]$^{+}$ clusters, it does perturb the spin mixture in favor of $S = 3/2$ form resulting in samples with 90% $S = 3/2$ and 10% $S = 1/2$ [4Fe-4S]$^{+}$ clusters.

In contrast to the mixed spin [4Fe-4S]$^{+}$ clusters found in frozen solution samples of the reduced WT Fd, the A33Y variant has exclusively $S = 3/2$ [4Fe-4S]$^{+}$ clusters as judged by analysis of the EPR spectrum shown in Fig. 1a. Moreover, the EPR properties were not perturbed by the addition of 50% (v/v) glycerol or 55% (v/v) PEG and the spectrum is readily interpreted in terms of a homogeneous $S = 3/2$ species. The EPR signal is the composite of two overlapping resonances with rhombic lineshapes, $g \sim 5.5$, 1.8, 1.3 and $g \sim 5.3$, 2.2, 1.6, that vary in relative intensity as a function of temperature. This is illustrated for the low-field component in Fig. 1b. The effective g-values of these doublets indicate that these are zero-field components of a rhombic $S = 3/2$ ground state $E/D = 0.30$, i.e. a perturbation treatment in the weak field limit ($D \gg h\nu$) using the conventional spin Hamiltonian shown above predicts doublets with $g = 5.50$, 1.80, 1.34 and $g = 5.32$, 2.16, 1.53, for $E/D = 0.30$ and $g_0 = 1.98$. An estimate of the energy separation between these doublets which corresponds to the zero-field splitting, Δ, was assessed by simulating the low-field component as the sum of two overlapping Gaussian-shaped bands and plotting the natural logarithm of the ratio of the intensities of the components centered at $g = 5.5$ and $g = 5.3$ versus $1/T$ (plot not shown). The resulting plot was a straight line to a good approximation and the slope (Δ/k) affords an estimate of $\Delta = 1.5 \pm 0.3$ and, thereby, an estimate of $D = -0.7 \pm 0.2$ cm^{-1}. This low value of D means that the assumption used in calculating the effective g-values based on the spin Hamiltonian, $D \gg h\nu$, may not be applicable. However, an exact calculation of the effective g-values using $E/D = 0.30$, $g_0 = 1.98$ and $D = -0.7$ cm^{-1} leads to doublets with $g = 5.43$, 1.82, 1.27, and $g = 5.23$, 2.14, 1.47, which are still in good agreement with the observed values. Hence the $S = 3/2$ ground states for the [4Fe-4S]$^{+}$ clusters in the WT and A33Y Fd differ markedly in terms of zero-field splitting parameters, $E/D = 0.22$ in WT versus 0.30 in A33Y and $D = +3.3$ cm^{-1} versus -0.7 cm^{-1} in A33Y.

3.3. VTMCD

The differences in the ground state parameters for the $S = 3/2$ [4Fe-4S]$^{+}$ clusters in the WT and A33Y Fd do not translate into significant differences in the excited state properties as assessed by VTMCD spectra, see Fig. 2. The VTMCD spectra show marked similarity and the only significant difference, i.e. the two weak negative bands centered around 620 nm and 680 nm in WT, is readily accounted for by contributions from the $S = 1/2$ [4Fe-4S]$^{+}$ clusters in the WT Fd. Extensive VTMCD studies of predominantly $S = 1/2$ and 3/2 [4Fe-4S]$^{+}$ clusters in nitrogenase Fe protein and synthetic analog complexes have shown that the major spectral difference lies in that $S = 1/2$ clusters have a broad and intense negative band centered between 580 and 680 nm while $S = 3/2$ clusters have

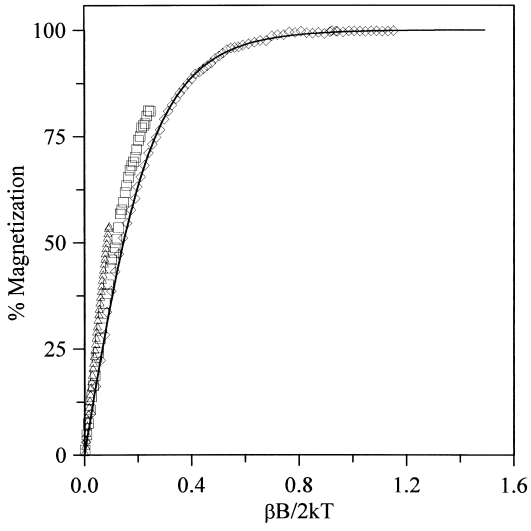

Fig. 3. MCD magnetization data for dithionite-reduced A33Y *P. furiosus* Fd. The sample is as described in Fig. 2. Magnetization data collected at 524 nm for magnetic fields between 0 and 6.0 T; temperatures (◇) 1.63 K, (□) 4.22 K, (△) 9.7 K. Solid line is theoretical magnetization data computed according to [25]) for an isolated doublet state with effective g-values, $g_{\parallel} = 5.51$, $g_{\perp} = 1.56$, and a polarization ratio, $m_z/m_{xy} = 0$.

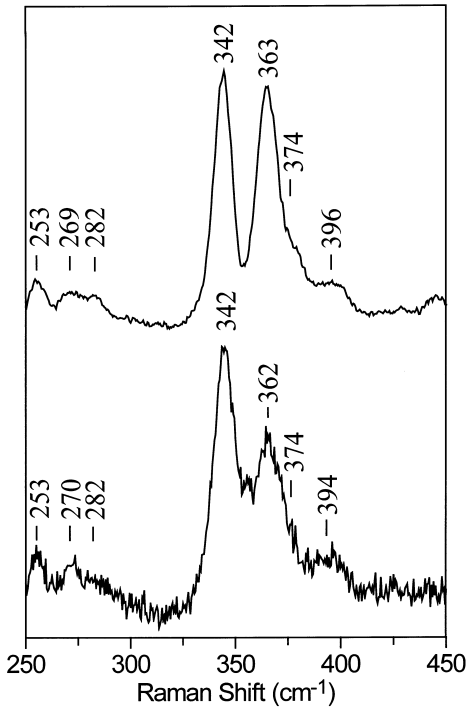

Fig. 4. Resonance Raman spectra of air-oxidized WT (top) and A33Y (bottom) *P. furiosus* 4Fe Fd with 457.9-nm excitation. Both spectra were recorded on samples (~1.5 mM) in 50 mM Tris-HCl buffer, pH 7.8, that were frozen at 28 K, with 75 mW laser power at the sample. Each scan involved photon counting for 1 s every 0.4 cm^{-1} for each scan; spectral resolution 8 cm^{-1}. For each spectrum the vibrational modes originating from the frozen buffer solution have been subtracted after normalizing the intensities of the 'ice-band' at 231 cm^{-1}, and a linear ramp fluorescence baseline was also subtracted. The WT and A33Y spectra shown are the sum of 25 and 21 scans, respectively.

little temperature-dependent MCD intensity in this region [7]. The generality of this difference in the VTMCD properties of $S = 1/2$ and 3/2 $[4Fe\text{-}4S]^+$ clusters has since been confirmed by studies of the pure $S = 3/2$ cluster in *P. furiosus* AOR [9] and the pure $S = 1/2$ $[4Fe\text{-}4S]^+$ clusters in D14C and D14C/C11S *P. furiosus* Fd [12,25]. The origin of this spectral difference is unclear at present and awaits detailed excited state electronic assignments for $S = 1/2$ and 3/2 $[4Fe\text{-}4S]^+$ centers.

MCD magnetization data for dithionite-reduced WT *P. furiosus* Fd were consistent with major contributions from a $S = 3/2$ component, but detailed analysis was not attempted due to the spin state heterogeneity [11]. A more detailed analysis was carried out for the more axial $S = 3/2$ cluster in *P. furiosus* AOR ($E/D = 0.12$ and $D = +4$ cm^{-1}) [9]. For temperatures below 2 K, when only the lowest doublet of the zero-field split ground state manifold is significantly populated, the data were fit to a good approximation by theoretical data, constructed according to published procedures [26], for an *xy*-polarized transition arising from an isolated doublet with the EPR-determined effective *g*-values, i.e. $g_\perp = 4.0$ and $g_\parallel = 2.0$. Although the zero-field splitting is much less for the more rhombic $S = 3/2$ $[4Fe\text{-}4S]^+$ cluster in A33Y Fd ($E/D = 0.30$, $D = 0.7$ cm^{-1}) and the population distribution over the lower and upper doublets of the $S = 3/2$ manifold is approximately 3:1 at 1.6 K, this procedure also affords satisfactory fits to the 1.6-K magnetization data collected at 524 nm, see Fig. 3. The lowest temperature data are simulated to a good approximation by theoretical data for an *xy*-polarized transition arising from an isolated doublet with effective *g*-values based on those experimentally determined for the lowest doublet, i.e. $g_\parallel = 5.51$ and $g_\perp = 1.56$. The success of this procedure in this case is likely to be a consequence of coalescence of the magnetization curves from each doublet as the ground state approaches maximal rhombicity ($E/D = 0.33$).

3.4. Resonance Raman

Resonance Raman provides a sensitive probe for structural perturbations in diamagnetic ($S = 0$) $[4Fe\text{-}4S]^{2+}$ clusters, but is of little use for $[4Fe\text{-}4S]^+$ clusters due to extremely poor enhancements of Fe-S stretching modes with visible excitation [27–29]. Detailed vibrational assignments under effective D_{2d} symmetry are available for biological $[4Fe\text{-}4S]^{2+}$ clusters, based on ^{34}S and ^{54}Fe isotope shifts, normal mode calculations and extensive studies of appropriate synthetic analog complexes [27], and these assignments have been extended to air-oxidized *P. furiosus* 4Fe Fd [11]. A comparison of the resonance Raman spectra of the $[4Fe\text{-}4S]^{2+}$ centers in WT and A33Y *P. furiosus* Fd obtained with 457.9-nm excitation is shown in Fig. 4. Apart from a slight broadening of the band centered at 362 cm^{-1}, the spectra are identical within experimental error attesting to negligible perturbation of the [4Fe-4S] core. Since the band at 362 nm has been primarily assigned to asymmetric Fe-S(Cys) stretching based on ^{34}S isotope shifts [11,30], the observed broadening is likely to result from small changes in cysteinyl Fe-S_γ-C_β-C_α dihedral angles and/or lowering the overall symmetry of the cluster environment as result of positioning a bulky tyrosyl residue in close proximity to the cluster. Resonance Raman spectra were recorded using 457.9-nm, 488.0-nm, and 514.5-nm excitation and in no case were the characteristic vibrations of an Fe-coordinated tyrosyl residue observed [31].

4. Discussion

EPR, VTMCD and resonance Raman investigations of the $[3Fe\text{-}4S]^+$ cluster assembled in the A33C variant of *P. furiosus* Fd revealed medium-dependent changes that have been interpreted in terms of ligation of the additional cysteine residue at position 33 [18]. In contrast, the spectroscopic results reported in this work for the A33Y variant show that a $[4Fe\text{-}4S]^{2+,+}$ cluster is assembled in the recombinant protein and give no indication of direct coordination of the cluster by the tyrosyl residue. Tyrosyl cluster coordination would be expected to be apparent by changes in the absorption and VTMCD spectra and the appearance of the characteristic resonance Raman bands of a coordinated tyrosine [31]; neither of which were observed. However, the spectroscopic and redox results show that positioning a tyrosyl residue in close proximity to the cluster alters both the midpoint potential of the $[4Fe\text{-}4S]^{2+,+}$ couple and the ground state properties of the $[4Fe\text{-}4S]^+$ cluster, without altering the excited state structure of the $[4Fe\text{-}4S]^+$ cluster or the core distortion of the $[4Fe\text{-}4S]^{2+}$ cluster.

Theoretical studies indicate that solvent exposure plays a major role in determining the electrostatic environment and thereby the midpoint potential of Fe-S clusters [32]. For example, the [4Fe-4S] cluster in high potential iron-sulfur proteins (HiPIPs) is enclosed by several hydrophobic aromatic side chains that restrict solvent accessibility and this is considered to be one of the key determinants for reducing the

midpoint potential of the [4Fe-4S]$^{3+,2+}$ couple so that it occurs within the physiological range and reducing the midpoint potential of the [4Fe-4S]$^{2+,+}$ couple so that it occurs outside of the physiological range. Hence it seems likely that the 38 mV decrease in potential that accompanies the A33Y mutation results from the tyrosyl residue limiting solvent exposure to the cluster.

Although there is as yet no detailed understanding of the factors that determine the ground state properties of $S = 3/2$ [4Fe-4S]$^{+}$ clusters, the results for the A33Y variant of *P. furiosus* Fd serve to demonstrate their sensitivity to protein environmental effects. For clusters with Fd-like arrangements of coordinating residues, the available data indicate that one oxygenic ligand (serinate or aspartate) is required to obtain $S = 3/2$ [4Fe-4S]$^{+}$ clusters in frozen solution. Comparison of the EPR properties of the WT and A33Y forms of *P. furiosus* Fd ($E/D = 0.22$ and 0.30, and $D = +3.3$ and -0.7 cm^{-1} for WT and A33Y, respectively) demonstrates that changes in immediate environment without any significant change in ligation or distortion in the cluster core can have a dramatic effect on the rhombicity, as well as the sign and magnitude of axial zero-field splitting of the $S = 3/2$ ground state. The [4Fe-4S]$^{+}$ centers in *P. furiosus* AOR and nitrogenase Fe proteins demonstrate that $S = 3/2$ ground states can arise for clusters with complete cysteinyl coordination, albeit in a non-Fd-like arrangement. Once again, differences in the cluster environment are manifest in dramatic differences in the ground state parameters, e.g. $E/D = 0.22$ and 0.12, and $D = -1.8$ and $+4.0$ cm^{-1}, for urea-treated *Azotobacter vinelandii* Fe protein [2,7] and *P. furiosus* AOR [9], respectively.

Thus far there are no well documented examples of biological [4Fe-4S]$^{+}$ clusters that exhibit $S = 3/2$ ground states at room temperature. The spin state of the cluster at room temperature can be assessed by magnetic susceptibility and/or NMR data and such data are only available for the nitrogenase Fe protein [33] and WT *P. furiosus* Fd [34]. In both cases, the available data point to homogeneous $S = 1/2$ ground states at room temperature and suggest that the $S = 3/2$ states are artifacts of freezing. However, the [4Fe-4S]$^{+}$ clusters in both these proteins exist as medium-dependent spin mixtures in frozen solutions [2,7] and the available structural data [35][1] indicate that the clusters are readily accessible to solvent. Hence organization of the solvent and glassing agent molecules in the vicinity of the cluster is likely to account for the spin state changes on freezing. Since the [4Fe-4S]$^{+}$ clusters in *P. furiosus* AOR [9] and the A33Y variant of *P. furiosus* Fd exhibit pure $S = 3/2$ ground states in frozen solutions with properties that are independent of medium effects, they represent the best candidates for clusters in which the $S = 3/2$ ground state is an intrinsic property as opposed to a freezing artifact. Magnetic susceptibility measurements using a SQUID magnetometer are planned to test this hypothesis. Moreover, the A33Y variant of *P. furiosus* Fd is amenable for detailed NMR, ^{57}Fe-ENDOR, Mössbauer and near-IR VTMCD studies to elucidate the intracluster valence delocalization and magnetic interactions that afford $S = 3/2$ rather than $S = 1/2$ ground states for [4Fe-4S]$^{+}$ clusters. This approach has already proven effective for understanding the origin of the $S = 1/2$ ground state of the [4Fe-4S]$^{+}$ clusters in WT, D14C and cyanide-bound *P. furiosus* Fd [17,36,37], and the stage is now set for extension to the $S = 3/2$ [4Fe-4S]$^{+}$ cluster in the A33Y variant.

Acknowledgements: This work was supported by a grant from the NIH (GM45597 to M.W.W.A. and M.K.J.) and an NSF Research Training Group Award to the Center for Metalloenzyme Studies (DBI-9413236). We thank Professor Fred Hagen for providing the results of an exact calculation of the effective g-values for $E/D = 0.30$, $g_0 = 1.98$ and $D = -0.7$ cm^{-1}.

References

[1] Hagen, W.R., Eady, R.R., Dunham, W.R. and Haaker, H. (1985) FEBS Lett. 189, 250–254.
[2] Lindahl, P.A., Day, E.P., Kent, T.A., Orme-Johnson, W.H. and Münck, E. (1985) J. Biol. Chem. 260, 11160–11173.
[3] Watt, G.D. and McDonald, J.W. (1985) Biochemistry 24, 7226–7231.
[4] Flint, D.H., Emptage, M.H. and Guest, J.R. (1992) Biochemistry 31, 10331–10337.
[5] Flint, D.H., Emptage, M.H., Finnegan, M.G., Fu, W. and Johnson, M.K. (1993) J. Biol. Chem. 268, 14732–14742.
[6] Onate, Y.A., Switzer, R.L., Vollmer, R.A. and Johnson, M.K. (1989) J. Biol. Chem. 264, 18386–18391.
[7] Onate, Y.A., Finnegan, M.G., Hales, B.J. and Johnson, M.K. (1993) Biochim. Biophys. Acta 1164, 113–123.
[8] Zambrano, I.C., Kowal, A.T., Adams, M.W.W., Mortenson, L.E. and Johnson, M.K. (1989) J. Biol. Chem. 264, 20974–20983.
[9] Koehler, B.P., Mukund, S., Conover, R.C., Dhawan, I.K., Roy, R., Adams, M.W.W. and Johnson, M.K. (1996) J. Am. Chem. Soc. 118, 12391–12405.
[10] George, S.J., Armstrong, F.A., Hatchikian, E.C. and Thomson, A.J. (1989) Biochem. J. 264, 275–284.
[11] Conover, R.C., Kowal, A.T., Fu, W., Park, J.-B., Aono, S., Adams, M.W.W. and Johnson, M.K. (1990) J. Biol. Chem. 265, 8533–8541.
[12] Brereton, P.S., Verhagen, M.F.J.M., Zhou, Z.-H. and Adams, M.W.W. (1998) Biochemistry 37, 7351–7362.
[13] Carney, M.J., Papaefthymiou, G.C., Spartalian, K., Frankel, R.B. and Holm, R.H. (1988) J. Am. Chem. Soc. 110, 6084–6095.
[14] Carney, M.J., Papaefthymiou, G.C., Whitener, M.A., Spartalian, K., Frankel, R.B. and Holm, R.H. (1988) Inorg. Chem. 27, 346–352.
[15] Arendsen, A.F., Hadden, J., Card, G., McAlpine, A.S., Bailey, S., Zaitsev, V., Duke, E.H.M., Lindley, P.F., Kröckel, M., Trautwein, A.X., Feiters, M.C., Charnock, J.M., Garner, C.D., Marritt, S.J., Thomson, A.J., Kooter, I.M., Johnson, M.K., van den Berg, W.A.M., van Dongen, W.M.A.M. and Hagen, W.R. (1998) J. Biol. Inorg. Chem. 3, 81–95.
[16] Aono, S., Bryant, D.A. and Adams, M.W.W. (1989) J. Bacteriol. 171, 3433–3439.
[17] Calzolai, L., Gorst, C.M., Bren, K.L., Zhou, Z.-H., Adams, M.W.W. and La Mar, G.N. (1997) J. Am. Chem. Soc. 119, 9341–9350.
[18] Duderstadt, R.E., Brereton, P.S., Adams, M.W.W. and Johnson, M.K. (1998) J. Am. Chem. Soc. 120, 8525–8526.
[19] Heltzel, A., Smith, E.T., Zhou, Z.-H., Blamey, J.M. and Adams, M.W.W. (1994) J. Bacteriol. 176, 4790–4793.
[20] Zhou, Z.-H. and Adams, M.W.W. (1997) Biochemistry 36, 10892–10900.
[21] Hagen, W.R. (1989) Eur. J. Biochem. 182, 523–530.
[22] Johnson, M.K. (1988) in: L. Que, Jr. (Ed.), Metal Clusters in Proteins, ACS Symposium Series, Vol. 372, American Chemical Society, Washington, DC, pp. 326–342.
[23] Thomson, A.J., Cheeseman, M.R. and George, S.J. (1993) Methods Enzymol. 226, 199–232.
[24] Drozdzewski, P.M. and Johnson, M.K. (1988) Appl. Spectrosc. 42, 1575–1577.
[25] Brereton, P.S., Duderstadt, R.E., Staples, C.R., Johnson, M.K. and Adams, M.W.W. (1999) Biochemistry, submitted.
[26] Bennett, D.E. and Johnson, M.K. (1987) Biochim. Biophys. Acta 911, 71–80.
[27] Czernuszewicz, R.S., Macor, K.A., Johnson, M.K., Gewirth, A. and Spiro, T.G. (1987) J. Am. Chem. Soc. 109, 7178–7187.
[28] Spiro, T.G., Czernuszewicz, R.S. and Han, S. (1988) in: T.G. Spiro (Ed.), Biological Applications of Raman Spectroscopy, Resonance Raman Spectra of Heme and Metalloproteins, Vol. 3, John Wiley and Sons, New York, pp. 523–554.

[29] Backes, G., Mino, Y., Loehr, T.M., Meyer, T.E., Cusanovich, M.A., Sweeney, W.V., Adman, E.T. and Sanders-Loehr, J. (1991) J. Am. Chem. Soc. 113, 2055–2064.
[30] Fu, W. (1990) M.S. Dissertation, University of Georgia.
[31] Que, Jr., L. (1988) in: T.G. Spiro (Ed.), Biological Applications of Raman Spectroscopy, Resonance Raman Spectra of Heme and Metalloproteins, Vol. 3, John Wiley and Sons, New York, pp. 491–521.
[32] Stephens, P.J., Jolie, D.R. and Warshel, A. (1996) Chem. Rev. 96, 2491–2513.
[33] Meyer, J., Gaillard, J. and Moulis, J.-M. (1988) Biochemistry 27, 6150–6156.
[34] Calzolai, L., Gorst, C.M., Zhou, Z.-H., Teng, Q., Adams, M.W.W. and La Mar, G.N. (1995) Biochemistry 34, 11373–11384.
[35] Georgiadis, M.M., Komiya, H., Chakrabarti, P., Woo, D., Kornuc, J.J. and Rees, D.C. (1992) Science 257, 1653–1659.
[36] Telser, J., Huang, H., Lee, H.-I., Adams, M.W.W. and Hoffman, B.M. (1998) J. Am. Chem. Soc. 120, 861–870.
[37] Johnson, M.K., Duin, E.C., Crouse, B.R., Golinelli, M.-P. and Meyer, J. (1998) in: E.I. Solomon and K.O. Hodgson (Eds.), Spectroscopic Methods in Bioinorganic Chemistry, ACS Symposium Series, Vol. 692, American Chemical Society, Washington, DC, pp. 286–301.